Check for updates

Article

INTERNATIONAL JOURNAL OF DAMAGE MECHANICS

International Journal of Damage Mechanics
2025, Vol. 34(6) 900–919
© The Author(s) 2024
Article reuse guidelines:
sagepub.com/journals-permissions
DOI: 10.1177/10567895241245865
journals.sagepub.com/home/ijd
Sage

Fracture mechanics approach to minimum reinforcement design of fibre-reinforced and hybrid-reinforced concrete beams

Alessio Rubino[1], Federico Accornero[2] and Alberto Carpinteri[2]

Abstract

The problem of the minimum reinforcement condition in fibre-reinforced and hybrid-reinforced concrete flexural elements is addressed in the framework of fracture mechanics by means of the Updated Bridged Crack Model (UBCM). The model describes the crack propagation process occurring in the critical cross-section of the reinforced member, by assuming the composite as a multiphase material, whereby the toughening contribution of the cementitious matrix and of the reinforcements are independently evaluated. The key-point of the discussion is that, when the influence of the matrix nonlinearities on the response is neglected, the minimum reinforcement condition is defined by a linear relationship between the critical values of two dimensionless numbers: (i) the *bar-reinforcement brittleness number*, N_P, proportional to the steel-bar area percentage, ρ; (ii) the *fibre-reinforcement brittleness number,* $N_{P,f}$, proportional to the fibre volume fraction, V_f. The model is applied to several experimental campaigns of the literature, in order to assess its suitability in the minimum reinforcement design of reinforced members in a unified fracture mechanics-based framework.

Keywords

Updated Bridged Crack Model, fibre-reinforced concrete, hybrid-reinforced concrete, minimum reinforcement condition, scale effects

Introduction

During the last fifty years, significant efforts have been made to understand the influence of fibres on the mechanical behaviour of cementitious materials, even in combination with traditional reinforcements. In the case of fibre-reinforced concrete (FRC), it is widely acknowledged that fibres provide post-cracking residual strength to the composite, with a consequent increase in its fracture

[1]Dept of Structural, Geotechnical and Building Engineering, Politecnico di Torino, Turin, Italy
[2]Dept of Civil Engineering and Intelligent Construction, Shantou University, Shantou, P.R. China

Corresponding author:
Alessio Rubino, Politecnico di Torino, Corso Duca degli Abruzzi, 24, Turin 10129, Italy.
Email: alessio.rubino@polito.it

energy which can be two orders of magnitude higher than that of plain concrete (Barros and Sena Cruz, 2001).

More precisely, the flexural response can be described by sub-dividing it into three different stages, as schematically represented in Figure 1. Stage I reflects the elastic behaviour of the FRC specimen prior to crack propagation. At the onset of the fracturing process, a slight decrease in the carried load is typically observed, which precedes the full activation of the reinforcements' bridging action in the post-cracking regime (Stage II) of the response. The latter can range from softening to pseudo-hardening depending, among other parameters, on the amount of reinforcing fibres (Liao et al., 2016). In any case, the flexural response is eventually characterized by a softening tail (Stage III) which is due to the pull-out of the short reinforcements at the critical cross-section of the specimen, where the damage is localized.

When fibres are used in combination with steel bars, i.e., in the case of hybrid-reinforced concrete (HRC) beams, the flexural behaviour of the composite depends on the amount of both the reinforcing phases. In the case of over-reinforced concrete beams, fibres significantly affect the crushing branch of the response, which become more stable due to the enhancement in the crushing energy of FRC (Mertol et al., 2015) (see upper curves in Figure 2). On the other hand, in the case of lightly-reinforced concrete beams, fibres affect the plastic plateau of the response, by increasing the load bearing capacity of the HRC specimen (Altun et al., 2007) (see lower curves in Figure 2). In addition to this, several experimental investigations pointed out a reduction in the deflection capacity of the HRC specimens (Colombo et al., 2023; Dancygier and Savir, 2006; Ning et al., 2015). This phenomenon can be justified considering the fibre enhancement in the bond behaviour at the rebar-concrete interface, which promotes earlier crack localization and possible bar rupture (Meda et al., 2012; Nguyen et al., 2019; Shao and Billington, 2020).

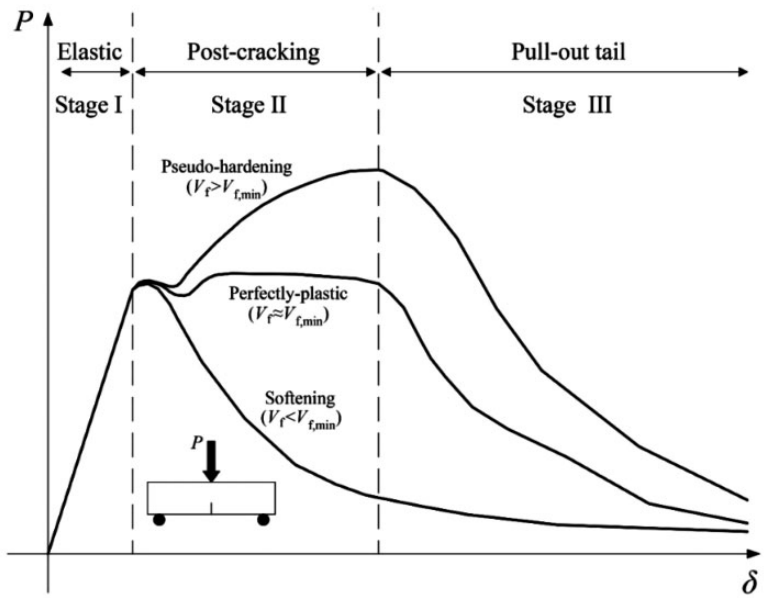

Figure 1. Influence of fibres on the flexural behaviour of FRC beams.

Despite the large amount of research work in this context, very few investigations aimed at defining the minimum reinforcement condition, i.e., the minimum amount of steel rebars and/or short fibres to guarantee the ultimate load of the specimen to be greater than the first cracking load.

In this respect, Naaman proposed a method to determine the minimum quantity of fibres to obtain multi-cracking phenomenon in unnotched FRC specimens subjected to tensile or flexural loading (Naaman, 2008). Considering a typical σ-ε curve, the critical fibre volume fraction, $V_{\mathrm{f,min}}$, was obtained by imposing the first cracking stress, σ_{cr}, equal to the ultimate post-cracking strength, σ_{u}:

$$V_{\mathrm{f,min}} = \frac{1}{1 + \frac{\tau}{\sigma_{\mathrm{mu}}}\frac{L}{d}(\lambda - \alpha)} \tag{1}$$

In equation (1), τ is the average value of the bond strength at the fibre-matrix interface, σ_{mu} is the tensile strength of the matrix, L/d is the fibre aspect ratio, whereas the coefficients λ and α take into account other effects, such as fibre orientation, fibre embedded length, group effect, etc. It is worth noting that the value of τ can be supposed or determined by means of pull-out tests carried out on the single fibre.

Similarly, the coefficients λ and α can be supposed a priori or identified by means of fracture surface analysis after experimental tests. Consequently, the application of this approach requires some hypotheses or extensive experimental campaigns in order to derive a reliable evaluation of $V_{\mathrm{f,min}}$.

More recently, Mobasher et al. (2015) proposed an analytical model to the design of HRC members. The cross-section model actually consists in an extension of a previous version, which was originally proposed to the design of FRC members. By assuming parametric constitutive laws to define the behaviour of the FRC matrix (intended as a unique phase) and of the ordinary reinforcements, strain compatibility and equilibrium conditions permit to describe the behaviour of FRC and HRC beams at the cross-section level in terms of moment vs curvature diagrams.

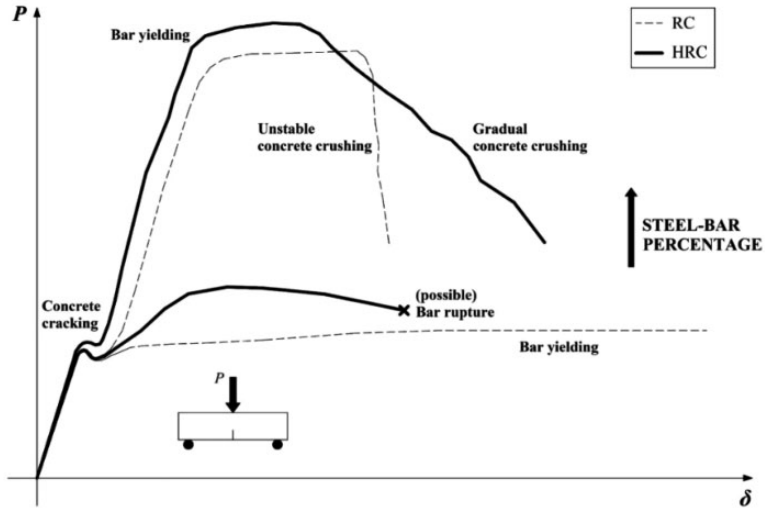

Figure 2. Influence of fibres on the flexural behaviour of HRC beams.

Following this route, by imposing the moment capacity equal to the first cracking moment, a linear relationship between the minimum steel-bar area percentage, ρ_{min}, and a parameter related to the post-cracking residual strength, μ, was found. In this sense, the model made evident the contribution of fibres to a partial (or total) replacement of bars at the minimum reinforcement condition for HRC members. Nevertheless, due to the assumption of the FRC composite as a mono-phase cementitious matrix, it was not possible to find an explicit relationship between ρ_{min} and $V_{f,min}$.

Another contribution was given by Fantilli et al. (2016), who proposed an analytical model, in which the ductile-to-brittle transition in the flexural response of FRC and HRC specimens was synthetically described by the so-called *ductility index*, *DI*, defined as follows:

$$DI = \frac{P_u - P_{cr}}{P_{cr}} = \frac{M_u - M_{cr}}{M_{cr}} \tag{2}$$

in which P_u is the ultimate load, P_{cr} is the cracking load, whereas M_u and M_{cr} are the corresponding bending moments. By assuming a linear relationship between *DI* and the reinforcing ratio, defined as $r = A_s/A_{s,min} + V_f/V_{f,min}$, the minimum reinforcement condition ($DI = 0$) was described by a linear relationship connecting the minimum amount of steel area, $A_{s,min}$, to the minimum amount of fibres, $V_{f,min}$. A consistent assessment of the latter quantities was possible by means of a design-by-testing procedure, on the basis of experimental flexural tests.

In all cases, the above-described approaches need to be accompanied by experimental testing in order to provide an effective prediction of the minimum reinforcement condition for structural applications. Moreover, the models are not able to predict any size-scale effect on the post-cracking behaviour of the composite structure, leaving a sort of uncertainty and unsafety in the passage from laboratory-scale specimens to full-scale structural elements.

The extensive research and, most importantly, the introduction of common standards (ACI Committee 544, 2018; FIB (Federation International du Bèton), 2012; RILEM TC 162-TDF, 2002, 2003) to the design of FRC structural members, have increasingly promoted the use of FRC in civil engineering, both as stand-alone application or in combination with ordinary reinforcement. Actually, the use of fibres —steel and synthetic macrofibres are typically employed— as the unique reinforcing phase is still limited to secondary members, e.g., slabs on grade, fibre shotcrete, and precast members (Di Prisco et al., 2009). On the other hand, the use of fibres in combination with traditional steel bars is typically preferred in truly structural applications, e.g., portal frames, multi-story buildings.

Focusing on the minimum reinforcement condition, both RILEM Recommendations and FIB Model Code, referring to hybrid reinforced structures, acknowledge that the presence of fibres provides a reduction in the minimum amount of steel-bar reinforcement required to contain the crack width in Serviceability Limit States (SLS). On the other hand, no information is given regarding the amount of fibres necessary to replace a given quantity of steel bars, in order to obtain a stable post-cracking response (load-bearing capacity greater than the cracking load) at Ultimate Limit States (ULS). In both cases, i.e., SLS and ULS, an explicit expression to quantitatively determine the influence of fibres on the minimum amount of steel bars is not provided.

In the present paper, the minimum reinforcement condition for FRC and HRC beams is discussed in the framework of Fracture Mechanics by means of the Updated Bridged Crack Model (UBCM). The model (Accornero et al., 2022c; Bosco and Carpinteri, 1995; Carpinteri, 1981, 1984; Carpinteri and Carpinteri, 1984; Carpinteri and Massabò, 1996, 1997a, 1997b; Carpinteri and Accornero, 2019, 2020) has been recently updated with new constitutive laws by the authors,

making it suitable to the case of steel fibre-reinforced (Accornero et al., 2022a; Carpinteri et al., 2022; Accornero et al., 2022d) and hybrid-reinforced (Accornero et al., 2022a; Rubino et al., 2023) concrete elements. In this work, further applications are shown providing a quantitative assessment of the minimum reinforcement condition with respect to different experimental campaigns of the literature, thus providing a unified framework for the minimum reinforcement design of FRC and HRC beams.

Nonlinear fracture mechanics models for cementitious materials

For a given material, the total strain energy release rate due to crack propagation, $G_{\mathrm{I,tot}}$, can be written as (Jenq and Shah, 1985):

$$G_{\mathrm{I,tot}} = G_{\mathrm{IC}} + G_{\mathrm{F}} = \frac{K_{\mathrm{IC}}^2}{E} + \int_0^{w_{\mathrm{u}}} \sigma(w)\mathrm{d}w \tag{3}$$

The first toughening contribution, G_{IC}, quantifies the energy dissipation due to the stress intensification occurring at the crack tip (Figure 3). In according to Linear Elastic Fracture Mechanics (LEFM) concepts, $\mathrm{G_{IC}}$ is connected to the fracture toughness of the material, K_{IC}, and its Young's modulus, E, via the Irwin's theorem: $G_{\mathrm{IC}} = \frac{K_{\mathrm{IC}}^2}{E}$. On the other hand, the second toughening contribution, G_{F}, relates to the energy consumption due to the closing stresses acting in the damage zone ahead of the crack tip, i.e., the so-called *fracture process zone* (Figure 3). Consistently with the *fictitious crack model* proposed by Hillerborg et al. (1976), it can be calculated as the area beneath the cohesive law of the material, $G_{\mathrm{F}} = \int_0^{w_{\mathrm{u}}} \sigma(w)\mathrm{d}w$, where σ_{u} and w_{u} represent the tensile strength and the critical crack opening of the material, respectively. In this sense, the toughening contribution related to G_{F} quantifies the influence of the material nonlinearities on the crack propagation process.

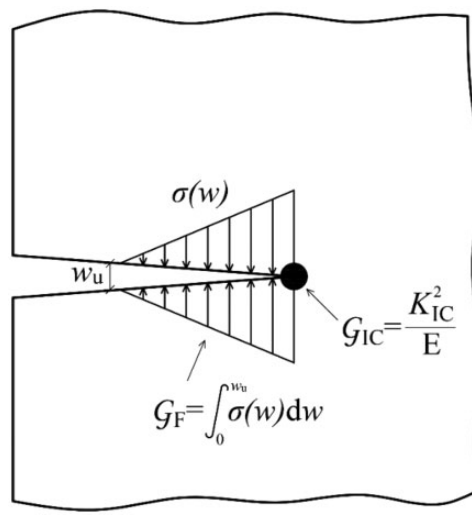

Figure 3. Energy dissipation required by crack propagation.

Depending on the material under investigation and on the characteristic specimen size, one of the two toughening contributions, related to K_{IC} and G_F respectively, can prevail on the other. For materials characterized by a high ratio σ_u/K_{IC} or in the case of very large specimens, the size of the developing fracture process zone remains small with respect to the characteristic specimen size. It happens for materials such as glass, high-strength steel, which are typically modelled in the framework of LEFM. Following this route, the singular crack-tip stress field is described by a global stress-intensity factor, K_I, thus neglecting the influence of the material nonlinearities on the crack propagation process. The crack propagates when K_I reaches the material fracture toughness, K_{IC} (*bridging option* (Carpinteri and Massabò, 1996)), the latter becoming the relevant fracture parameter with respect to G_F.

On the other hand, when the material is characterized by a low ratio σ_u/K_{IC}, or in the case of small specimens, the size of the developing fracture process zone, together with its influence on the crack propagation process, cannot be ignored. This happens for cementitious materials, such as cement paste, mortar, and concrete, for which the remarkable influence of the material nonlinearities on the fracture behaviour is clearly observed. Under these circumstances, a finite stress field is typically assumed, whereby the crack propagates when the maximum stress in the ligament reaches the material tensile strength, σ_u (*cohesive option* (Carpinteri and Massabò, 1996)). Following this route, the influence of the stress intensification at the crack tip is not considered, whereas G_F becomes the relevant fracture parameter with respect to K_{IC}.

In the case of reinforced composite materials, a further toughening contribution, which is additional to that of the matrix (equation (3)), comes into play due to the presence of the reinforcing elements such as short fibres, continuous bars, rods, particles, whiskers, etc. This contribution can be related to different bridging mechanisms (debonding, slippage, yielding and/or reinforcement rupture) which can occur as a function of the properties at the matrix-reinforcement interface and of the reinforcement length.

Focusing on civil engineering applications, let us consider the case of cementitious-based composites, in which the reinforcing phase can be made of continuous bars (ordinary reinforced concrete, RC), short fibres (fibre-reinforced concrete, FRC), or a combination of them (hybrid-reinforced concrete, HRC). In all cases, it is widely acknowledged that the nonlinear contribution in the mechanical response of the composite is mainly due to the reinforcing phases compared to the cementitious matrix, despite the quasi-brittle behaviour of the latter. This makes reasonable to neglect the energy dissipation in the matrix fracture process zone (G_F in equation (3)), thus assuming the matrix as a linear elastic-perfectly brittle mean, whose fracture resistance is characterized solely by its fracture toughness, K_{IC}. This is the key-assumption of the basis of the fracture mechanics approach that is presented in the following.

Updated Bridged Crack Model (UBCM)

The Updated Bridged Crack Model (UBCM) focuses on the crack propagation process occurring in the critical cross-section of reinforced composites. In the framework of UBCM, the composite is interpreted as a multi-phase material, in which the matrix and the reinforcing elements (continuous bars, short fibres, etc.) represent the primary and secondary phase of the mixture, respectively. Following the above-discussed assumptions (bridging option), the matrix is assumed as linear elastic-perfectly brittle mean, whose toughening contribution is defined by the matrix fracture toughness, K_{IC}. On the other hand, the toughening contribution of the reinforcing phases is modelled by a distribution of closure forces which bridge the crack faces.

The problem is geometrically defined in Figure 4, where the reinforced cross-section is characterized by the thickness, b, the depth, h, the initial edge crack depth, a_0, and it is subjected to an external bending moment, M. A distribution of reinforcing layers—each one placed at a distance c_i from the bottom edge of the beam—is considered.

The cross-section analysis requires some preliminary information regarding the reinforcing elements. Firstly, the total number of reinforcing elements crossing the critical cross section and their position have to be defined. In this respect, it is worth noting that the number of steel rebars and their position are generally known in the geometric design of the reinforced concrete element. On the other hand, the number of short fibres, n, is unknown because of their random distribution within the structural member. It can be calculated as:

$$n = \alpha V_{\mathrm{f}} \frac{bh}{A_{\mathrm{f}}} \tag{4}$$

where n is related to the theoretical number of fibres in the cross section ($V_{\mathrm{f}} bh/A_{\mathrm{f}}$) via the so-called orientation factor, α (Robins et al., 2003). In equation (4) A_{f} represents the cross-section area of the reinforcing fibre.

Moreover, it is useful to note that the bridging force of the i-th active reinforcement can be put in connection with the tensile stress active in the reinforcing element, σ_i, via the so-called snubbing coefficient, β_i (Li et al., 1990):

$$F_i = \beta_i \sigma_i A_i \tag{5}$$

In equation (5) A_i indicates the cross-section area of the reinforcing element. The coefficient β_i incorporates some secondary effects related to the orientation of the reinforcements with respect to the crack faces. In the case of continuous reinforcements, such as steel rebars, it is implicitly equal to one.

Following these considerations, the cross-section analysis is based on the following analytical conditions: (i) *crack propagation condition*, which is defined in the framework of Linear Elastic

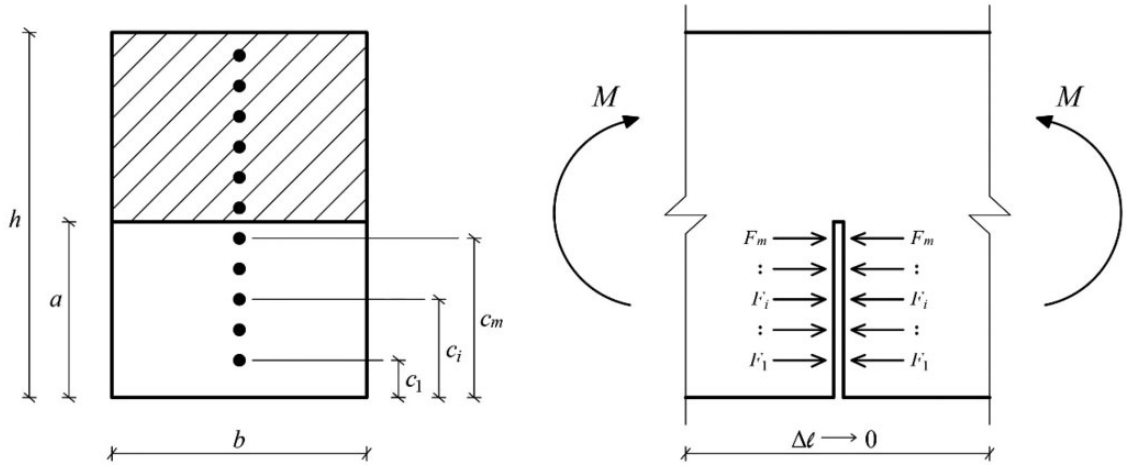

Figure 4. UBCM modelling of the reinforced cross-section.

Fracture Mechanics (LEFM), whereby the crack propagates when the global stress-intensity factor, K_I, reaches the matrix fracture toughness, K_{IC} (equation (6)); (ii) *reinforcement constitutive laws*, which provide a direct connection between the reinforcement bridging force, F, and the corresponding crack opening displacement, w (equation (7)); (iii) *displacement compatibility conditions*, whereby the crack opening at each reinforcement level, w, is calculated as a function of the applied bending moment, M, and of the bridging forces distribution (equation (8)):

$$K_I = K_{IM} - \sum_{i=1}^{m} K_{IF,i} = \frac{M}{bh^{3/2}} Y_M - \frac{\{Y_F\}^T \{F\}}{bh^{1/2}} = K_{IC} \tag{6}$$

$$\{F\} = \{F(w)\} \tag{7}$$

$$\{w\} = \{\lambda_M\} M - [\lambda]\{F\} \tag{8}$$

The UBCM numerical algorithm has general validity, i.e., it is able to describe the cracking behaviour of any composite as long as appropriate constitutive laws (equation (7)) are used to describe the actual bridging mechanisms of the reinforcements, which can include their slippage, yielding, or even rupture. Among them, one mechanism can prevail on the other as a depending on the reinforcement strength, on the bonding condition at the reinforcement-matrix interface, and on the anchorage length.

In the case of continuous bars, the reinforcement slippage is typically avoided by means of ribs along the longitudinal profile of the reinforcement and adequate anchorage length, in order to fully exploit the mechanical resistance (yielding) of the reinforcement. This is the case of steel rebars, whereby an hardening-perfectly plastic law can be used to describe the yielding mechanism of the reinforcement (Figure 5(a)). On the other hand, in the case of short reinforcements, e.g., fibres, the anchorage (embedded) length of the reinforcement is sufficiently small so that fibre pull-out occurs. Under these circumstances, a softening law is suggested to describe the reinforcement bridging mechanism (Figure 5(b) and (c) for straight and hooked-end steel fibres).

Equations (6) to (8) constitute the core of the UBCM numerical algorithm, thus resulting in a system of $2m+1$ analytical conditions (equilibrium, constitutive, and kinematic) in $2m+1$ unknowns, i.e., the profile of the crack opening displacements, $\{w\}$, the corresponding distribution of bridging forces, $\{F\}$, and the fracturing moment, M_F. The solution is obtained by means of a numerical iterative procedure (Crack Length Control Scheme), whose steps are represented in the flowchart of Figure 6.

Considering the response at the cross-section level, the fracture moment, M_F, represents the static parameter of the response, whereas the local rotation, φ, represents its kinematic counterpart. The latter can be calculated as:

$$\varphi = \lambda_{MM} M - \{\lambda_M\}^T \{F\} \tag{9}$$

The corresponding specimen deflection, δ, can be obtained by applying the superposition principle, by which the total deflection takes into account both the inelastic contribution related to the fracturing process in the critical section (inelastic hinge) and that related to the elastic behaviour of the remaining part of the beam. Following this route, it is possible to describe the composite flexural response at the cross-section level, i.e., in terms of fracture moment vs local rotation ($M_F-\varphi$) diagrams or, alternatively, at the specimen level, i.e., in terms of load vs deflection ($P-\delta$) diagrams.

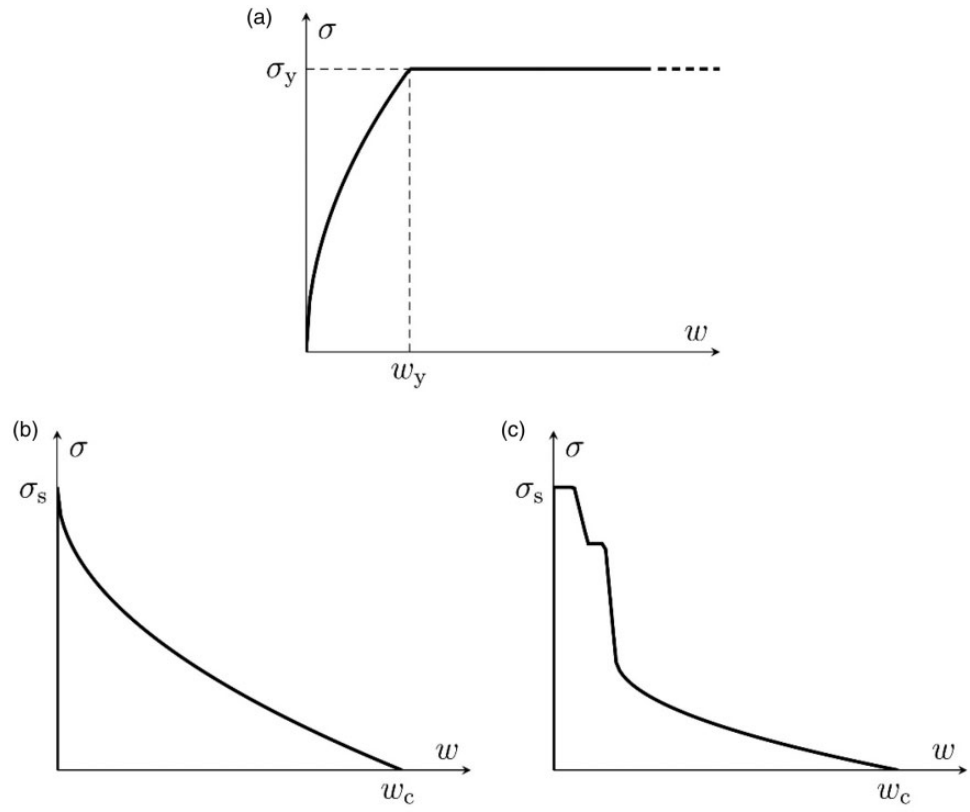

Figure 5. Reinforcement constitutive laws: (a) Continuous steel bars; (b) Straight steel fibres and (c) Hooked-end steel fibres.

Dimensionless numbers and minimum reinforcement condition

Under the abovementioned assumptions, UBCM is able to predict different flexural responses as a function of three dimensionless numbers (Accornero et al., 2022a; Rubino et al., 2023), i.e., the *bar-reinforcement brittleness number*, N_P, the *fibre-reinforcement brittleness number*, $N_{P,f}$, and the *pull-out brittleness number*, N_w, which are defined as follows:

$$N_P = \rho \frac{\sigma_y}{K_{IC}} h^{1/2} \tag{10}$$

$$N_{P,f} = V_f \frac{\sigma_s}{K_{IC}} h^{1/2} \tag{11}$$

$$N_w = \frac{E w_c}{K_{IC} h^{1/2}} \tag{12}$$

The *reinforcement brittleness numbers*, N_P and $N_{P,f}$, are dependent on the amount of the related reinforcing phases, on the corresponding ultimate stress (yielding strength for continuous bars, σ_y,

and slippage strength for short fibres, σ_s), on the matrix fracture toughness, K_{IC}, and on the characteristic structural size (beam depth), h. The latter comes into play to balance the mismatch between the physical dimensions of a generalized strength ($[F][L]^{-2}$) and those of a fracture toughness ($[F][L]^{-3/2}$) (Carpinteri and Accornero, 2021). Eventually, *the pull-out brittleness number*, N_w, depends on the matrix Young's modulus, E, on the equivalent (average) embedded length of the fibre-reinforcement, w_c, on the matrix fracture toughness, K_{IC}, and on the beam depth, h.

As extensively discussed by the authors in recent research works (Accornero et al., 2022a, 2022c, 2022d; Carpinteri et al., 2022; Rubino et al., 2023), all the three dimensionless numbers play a key-role in the stability of the fracturing process occurring in the critical cross-section. N_P and $N_{P,f}$ have a direct influence on the load bearing capacity of the composite. More precisely, N_P defines the level

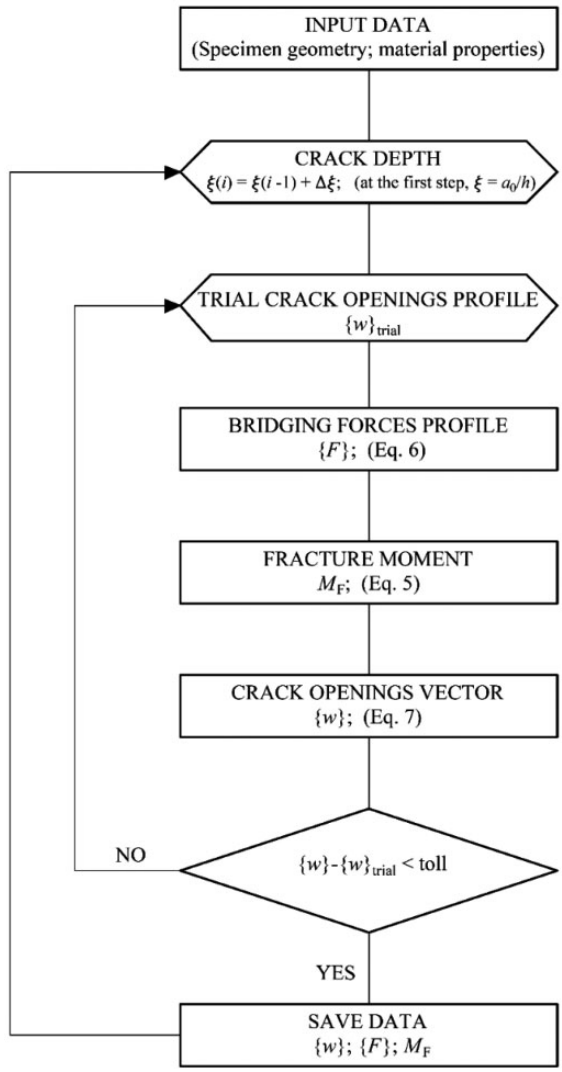

Figure 6. Flowchart of the UBCM numerical algorithm.

of the final plastic plateau, whereas $N_{P,f}$ contributes to the flexural capacity in the intermediate stage of the flexural response (Figure 7(a) and (b)). Eventually, N_w controls the exhaustion of the fibre toughening contribution in the final stage of the response, with a direct influence on the inelastic rotation capacity of the cross-section (Figure 7(c)).

In this paper, the focus is on the minimum reinforcement condition, which is meant to be obtained when the ultimate bending moment, M_u, is equal to the first cracking bending moment, M_{cr}, which occurs at the onset of the fracturing process.

The dimensionless first cracking moment, $\tilde{M}_{cr}$, (indicated by a red square marker in Figure 7), is independent on the dimensionless numbers. In the framewok of UBCM, it can be defined in closed-form analytical expression as a function of the dimensionless initial notch depth, a_0/h:

$$\frac{M_{cr}}{K_{IC} b h^{3/2}} = \tilde{M}_{cr} = \frac{1}{Y_M(a_0/h)} \tag{13}$$

In Figure 8 the dimensionless first cracking moment, $\tilde{M}_{cr}$, is plotted against a_0/h, for a_0/h ranging from 0 (unnotched specimen) to 0.60. It is worth noting that, consistently with LEFM, equation (13)

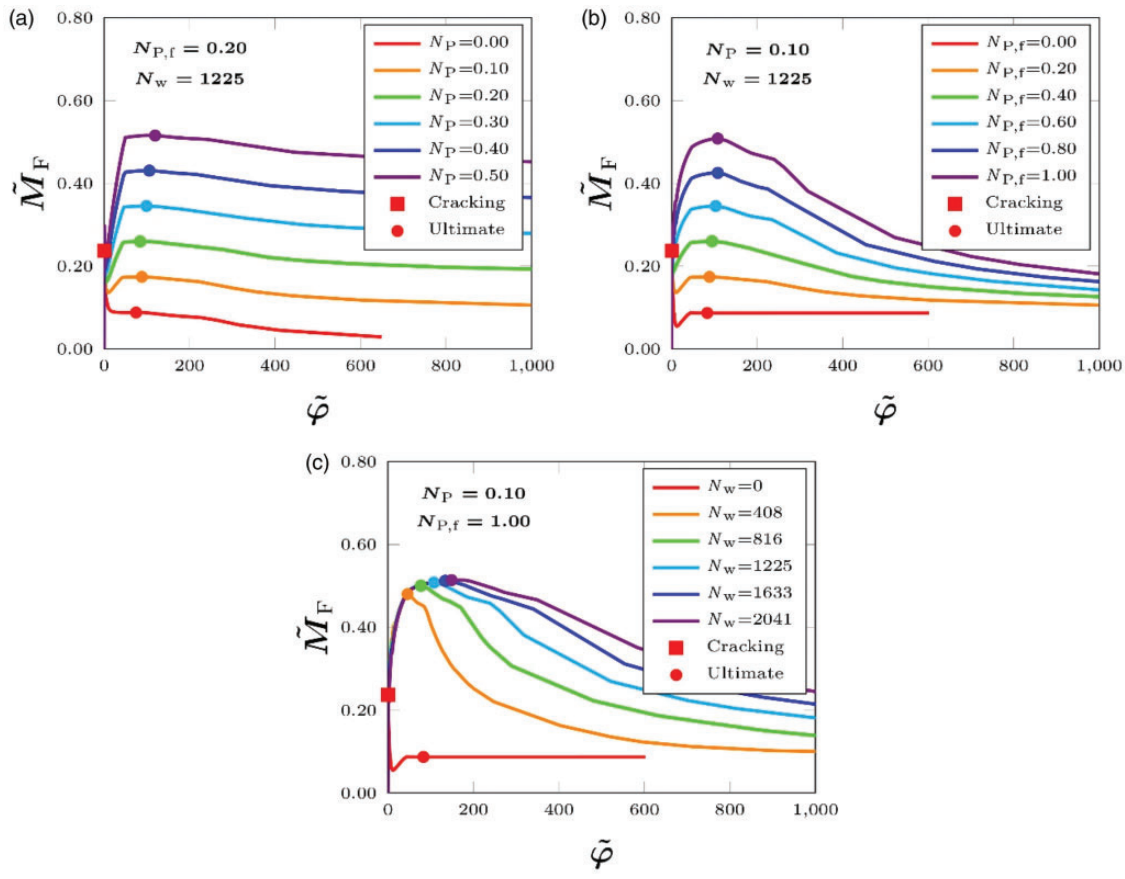

Figure 7. UBCM numerical simulations for HRC beams: (a) Influence of N_P; (b) Influence of $N_{P,f}$ and (c) Influence of N_w.

is affected by a singularity in the case of unnotched specimens ($a_0/h = 0$), whereby $\tilde{M}_{cr}$ tends to infinity. This problem can be overcome by introducing a cut-off (fictitious notch) to provide an effective assessment of the first cracking moment of initially smooth specimens.

On the other hand, the dimensionless ultimate bending moment, $\tilde{M}_u$, is measured in the post-cracking stage of the flexural response. $\tilde{M}_u$ is found to depend on both the reinforcement brittleness

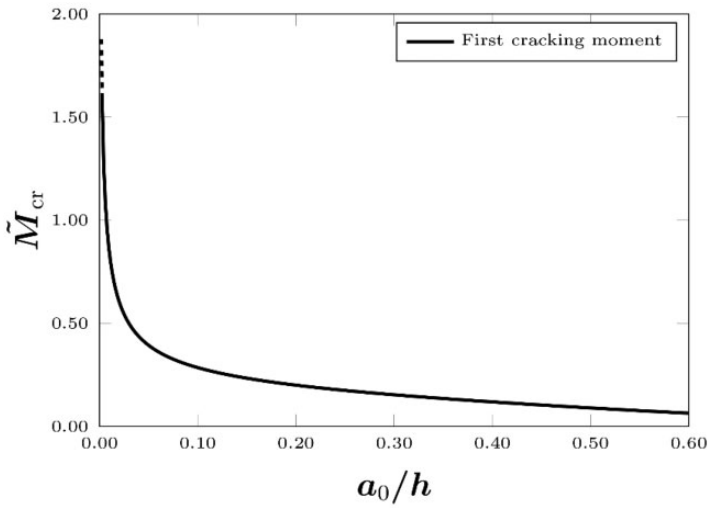

Figure 8. First cracking moment, $\tilde{M}_{cr}$, vs initial crack depth, a_0/h.

Table 1. Identified mechanical parameters and minimum reinforcement condition.

Reference	K_{IC} (MPa mm$^{1/2}$)	σ_y (MPa)	σ_s (MPa)	w_c (mm)	ρ (%)	V_f (%)	N_P (−)	$N_{P,f}$ (−)	N_w (−)
Almusallam et al. (2016)	47	–	326	26.1	0	1.20	0	1.02	1815
						1.40		1.19	
Barros et al. (2003)	36	–	244	15.3	0	0.32	0	0.27	1136
						0.95		0.79	
Barros et al. (2005)	28	–	297	23.6	0	0.13	0	0.17	2343
						0.26		0.34	
						0.39		0.51	
Bencardino et al. (2010)	44	–	306	17.5	0	1.00	0	0.85	1322
						2.00		1.70	
Mobasher et al. (2014)	17	–	199	25	0	0.16	0	0.23	3638
						0.33		0.47	
						0.50		0.70	
Gorino and Fantilli (2020)	27	527	305	15	0.13	0.50	0.30	0.69	1450
						0.75		1.04	
Holschemacher et al. (2010)	64	800	462	10	0.25	0.25	0.38	0.22	531
						0.51		0.45	
						0.76		0.66	
Mobasher et al. (2015)	20	560	295	9.5	0.25	0.32	1.00	0.67	1068
					0.56	0.64	2.24	1.34	

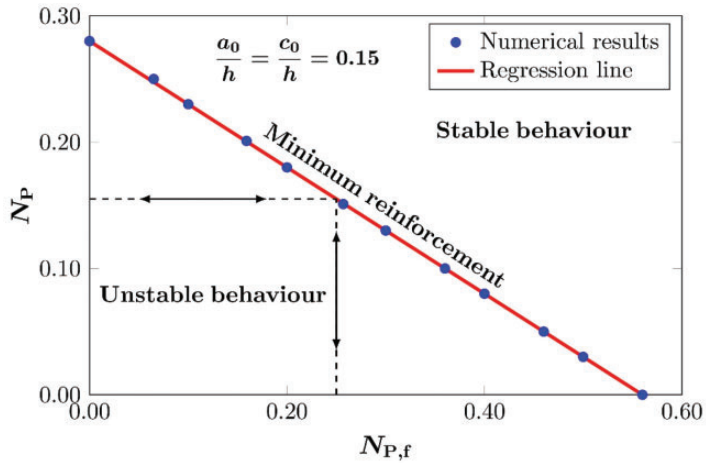

Figure 9. Minimum reinforcement design nomograph.

Table 2. UBCM minimum reinforcement predictions.

Reference	ρ_{min} (%)	$V_{f,min}$ (%)
Almusallam et al. (2016)	–	0.63
Barr et al. (2003)	–	0.64
Barros et al. (2005)	–	0.41
Bencardino et al. (2010)	–	0.62
Mobasher et al. (2014)	–	0.58
Gorino et al. (2020)	0.19	0.61
Holschemacher et al. (2010)	0.19	0.63
Mobasher et al. (2015)	0.11	0.41

numbers, N_P and $N_{P,f}$, whereas the influence of N_w and a_0/h is negligible. In a general form, it can be written:

$$\frac{M_u}{K_{IC} b h^{3/2}} = \tilde{M}_u = f(N_P, N_{P,f}) \tag{14}$$

Actually, by means of UBCM numerical simulations it can be proved that $\tilde{M}_u$ is linearly dependent on N_P and $N_{P,f}$, thus implying a linear relationship between the ultimate bending moment and the amount of the corresponding reinforcing phases, ρ and V_f, respectively.

As a consequence of equations (13) and (14), the minimum reinforcement condition in FRC and HRC is synthetically described by a design nomograph in which the critical values of the reinforcement brittleness numbers, N_P and $N_{P,f}$, are linearly connected for a given value of the dimensionless initial crack depth, a_0/h, and of the concrete cover, c_0/h (Accornero et al., 2022a; Rubino et al., 2023). In Figure 9 the design nomograph refers to $a_0/h = c_0/h = 0.15$, but similar conclusions can be drawn for different values of a_0/h and c_0/h. In all cases, the red regression line defines the couples of

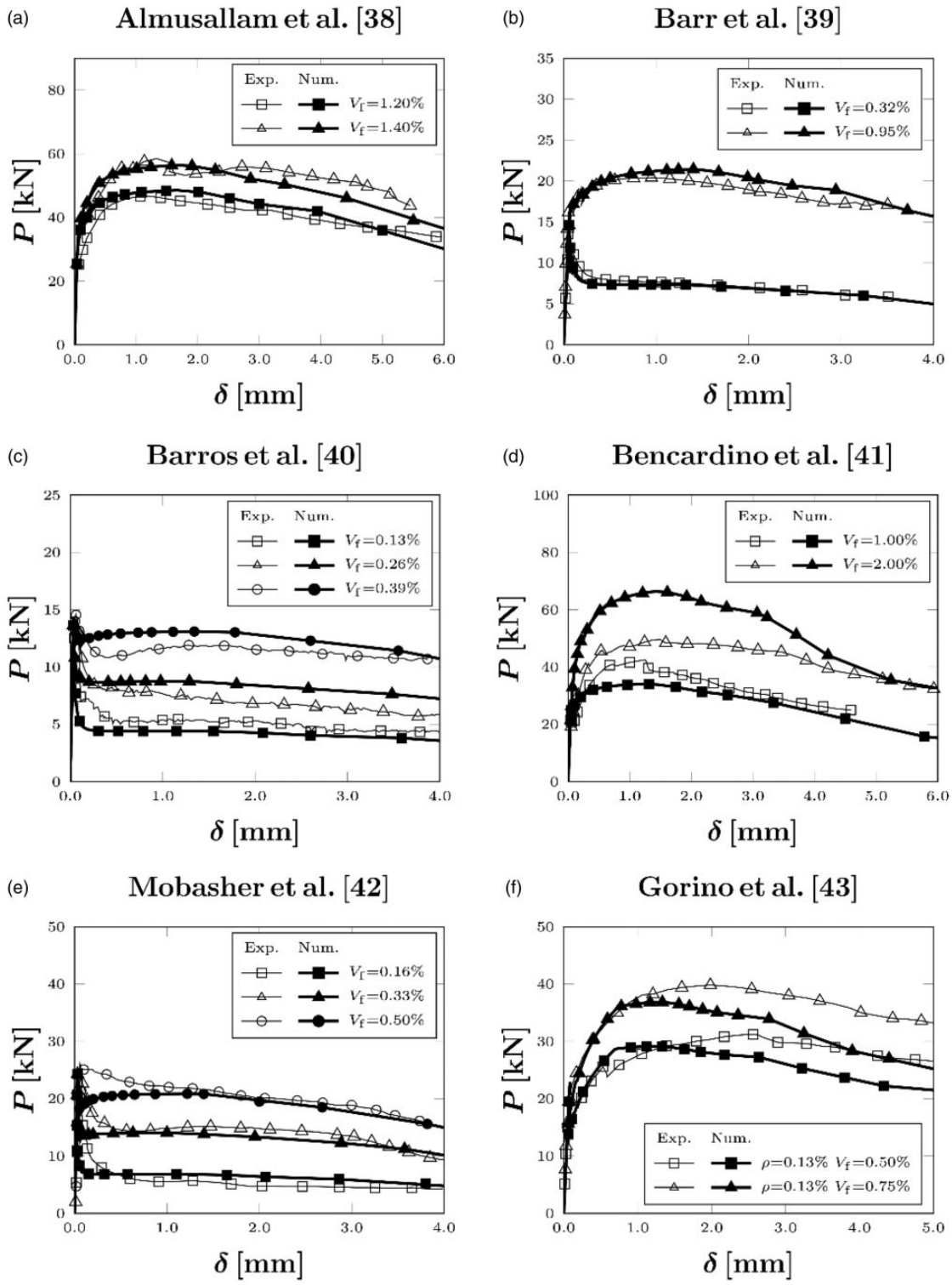

Figure 10. Experimental results vs UBCM numerical predictions for FRC and HRC beams.

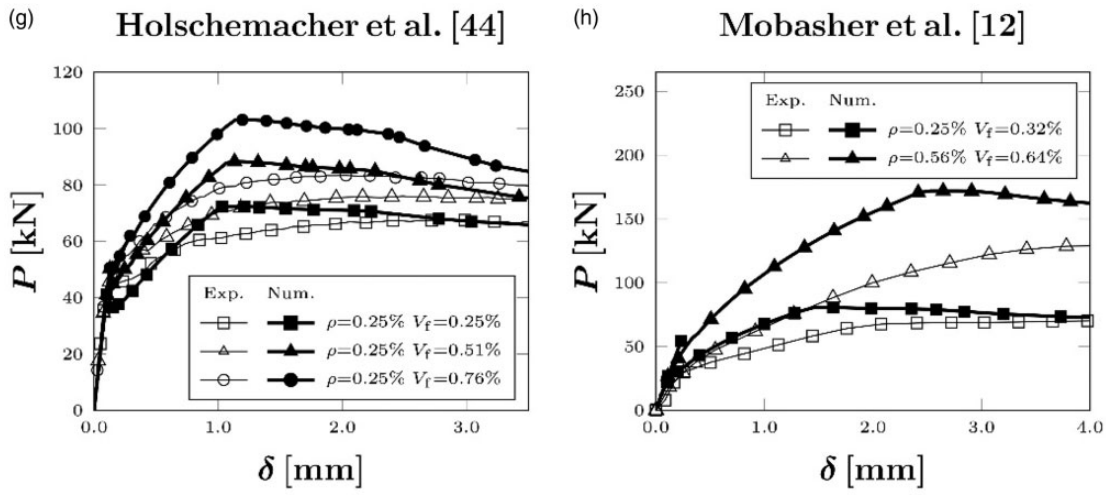

Figure 10. Continued.

critical values of N_P and $N_{P,f}$ for which a stable post-cracking response is guaranteed. All the other parameters being the same, the linear relationship of Figure 9 can be translated in the corresponding relationship between the minimum steel-bar area percentage, ρ_{min}, and the corresponding minimum fibre volume fraction, $V_{f,min}$.

Applications

In this section, the UBCM is applied to provide an assessment of the minimum reinforcement condition with reference to different experimental campaigns reported in the scientific literature, involving both FRC (Almusallam et al., 2016; Barr et al., 2003; Barros et al., 2005; Bencardino et al., 2010; Mobasher et al., 2014) and HRC (Mobasher et al., 2015; Gorino and Fantilli, 2020; Holschemacher et al., 2010) specimens.

The experimental tests included three-point bending (3PB) and four-point bending (4PB) tests on both notched and unnotched prismatic specimens. Cementitious matrices of different compression strengths and reinforced with different types of hooked-end steel fibres and/or steel rebars were taken into account. In all cases, the flexural behaviour was investigated as a function of the amount of the reinforcing phases, i.e, the steel-bar area percentage, ρ, and the fibre volume fraction, V_f.

Within each specimen group, the application of UBCM requires the identification of the constitutive parameters of the concrete matrix (fracture toughness, K_{IC}), of the steel bars (yielding strength, σ_y) and of the reinforcing fibres (slippage strength, σ_s, and fibre embedment length, w_c). The identification of these parameters has been carried out by applying the Pareto's approach on the basis of the experimental flexural curves, as already discussed by the authors in previous research works (Accornero et al., 2022a, 2022c, 2022d; Carpinteri et al., 2022; Rubino et al., 2023).

When the mechanical properties of the composite are defined, the model is able to predict the flexural response as a function of ρ and V_f, taken as unique variables. The latter proportionally affect the reinforcement brittleness numbers, N_P and $N_{P,f}$, by means of equation (10) and (11), whereas N_w remains constant, consistently with equation (12). The values of the identified

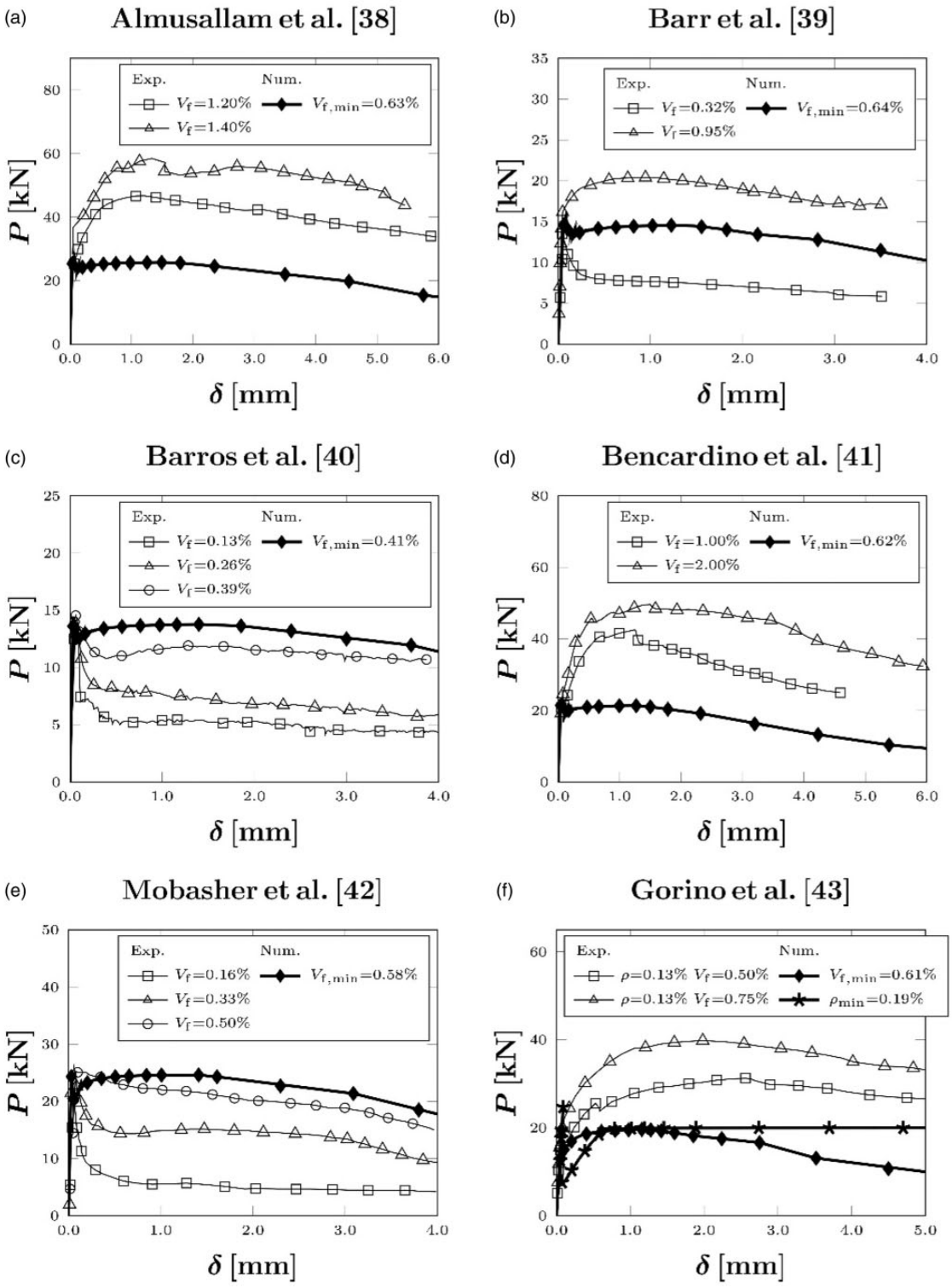

Figure 11. Experimental results vs UBMC minimum reinforcement predictions for FRC and HRC beams.

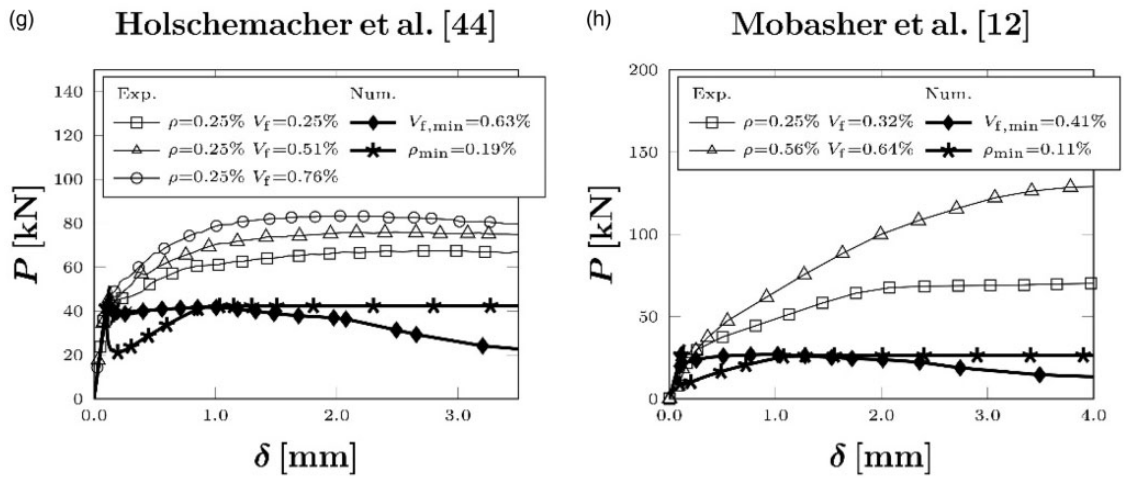

Figure 11. Continued.

constitutive parameters and of the brittleness numbers N_P, $N_{P,f}$, and N_w are reported in Table 1 for each specimen group under consideration.

In Figure 10, the superposition between the experimental curves and the UBCM numerical predictions is represented. In all cases, a consistent agreement is found, thus proving the capability of the model in predicting the transition in the flexural response of the reinforced specimens due to the variation in the amount of the reinforcing phases. Nevertheless, it is worth noting that in this case of FRC specimens the numerical predictions are almost overlapped to the experimental curves (Figures 10(a) to (e)), whereas a larger scatter is obtained in the case of HRC specimens (Figures 10(f) to (h)). This is due to the assumption of a simplified constitutive law of the steel bar (Figure 5(a)) which does not take into account the hardening behaviour beyond the yielding point of steel and, most importantly, the influence of fibres on the bond behaviour at the rebar-concrete interface. As a matter of fact, the adopted constitutive laws (Figure 5) are defined as independent of each other, thus neglecting the interaction between the two different reinforcing phases.

Considering the critical values of N_P and $N_{P,f,}$ the design nomograph of Figure 9 provides a quantitative evaluation of the minimum reinforcement for FRC and HRC beams in an unified framework.

In Table 2, the obtained values of $V_{f,min}$ and ρ_{min} are reported for each experimental campaign under consideration. It is worth noting that in the case of FRC specimens ((Almusallam et al., 2016; Barr et al., 2003; Barros et al., 2005; Bencardino et al., 2010; Mobasher et al., 2014)) only $V_{f,min}$ can be calculated, which results to be included between 0.41% and 0.64%, consistently with the experimental data. On the other hand, in the case of HRC specimens ((Mobasher et al., 2015; Gorino and Fantilli, 2020; Holschemacher et al., 2010)) infinite minimum reinforcement conditions, i.e., infinite combinations of $V_{f,min}$ and ρ_{min}, could be determined for each experimental investigation by using the design nomograph of Figure 9. For the sake of simplicity, two limit conditions are represented, corresponding to the case in which the minimum reinforcement is given only by means of steel bars or fibres, respectively. Considering Figure 9, they correspond to two points given by the intersection of the red regression line with the axes of the nomograph.

In Figure 11 the corresponding UBCM minimum reinforcement curves are represented together with the experimental curves, in order to show the effectiveness of the model predictions.

Conclusions

The Updated Bridged Crack Model (UBCM) is applied as a Fracture Mechanics tool to predict the minimum reinforcement condition in fibre-reinforced concrete (FRC) and hybrid-reinforced concrete beams (HRC) with respect to different experimental campaigns of the literature. The main features of the model are recalled, giving particular emphasis to the three *brittleness numbers*, N_P, $N_{P,f}$, and N_w, which govern the stability of the fracturing process. In the framework of the proposed model, the minimum reinforcement design is driven by a design nomograph which provides a linear relationship between the critical values of N_P and $N_{P,f}$, thus implying a relationship between the minimum steel-bar area percentage (ρ_{min}) and the minimum fibre volume fraction ($V_{f,min}$). It is shown that UBCM numerical predictions compares favorably with numerous experimental campaigns carried out on FRC and HRC specimens, thus providing a consistent evaluation of ρ_{min} and $V_{f,min}$ in an unified framework.

Declaration of conflicting interests

The author(s) declared no potential conflicts of interest with respect to the research, authorship, and/or publication of this article.

Funding

The author(s) disclosed receipt of the following financial support for the research, authorship, and/or publication of this article: Federico Accornero acknowledges the support from STU Outstanding Talent Grant N. 140-09423016.

ORCID iDs

Alessio Rubino https://orcid.org/0000-0002-7917-549X
Federico Accornero https://orcid.org/0000-0002-9638-8411

References

Accornero F, Carpinteri A and Rubino A (2022a) A fracture mechanics approach to the design of hybrid-reinforced concrete beams. *Engineering Fracture Mechanics* 275: 108821.

Accornero F, Rubino A and Carpinteri A (2022b) Ductile-to-brittle transition in fiber-reinforced concrete beams: Scale and fiber volume fraction effects. *Material Design & Processing Communication* 2(6): 1–11. DOI:10.1002/mdp2.127.

Accornero F, Rubino A and Carpinteri A (2022c) Post-cracking regimes in the flexural behaviour of fibre-reinforced concrete beams. *International Journal of Solids and Structures* 248: 111637.

Accornero F, Rubino A and Carpinteri A (2022d) Ultra-low cycle fatigue (ULCF) in fibre-reinforced concrete beams. *Theoretical and Applied Fracture Mechanics* 120: 103392.

ACI Committee 544 (2018) ACI PRC-544.4-18: Guide to design with fiber-reinforced concrete. American Concrete Institute (ACI). Farmington Hills, MI.

Almusallam T, Ibrahim SM, Al-Salloum Y, et al. (2016) Analytical and experimental investigations on the fracture behaviour of hybrid fiber reinforced concrete. *Cement and Concrete Composites* 74: 201–217.

Altun T, Haktanir T and Ari K (2007) Effects of steel fibre addition on mechanical properties of concrete and RC beams. *Construction and Building Materials* 21(3): 654–661.

Barr BIG, Lee MK, de Place Hanses EJ, et al. (2003) Round-robin analysis of the RILEM TC 162-TDF beam-bending test: Part 1 – Test method evaluation. *Materials and Structures* 36(9): 609–620.

Barros JOA and Sena Cruz J (2001) Fracture energy of steel fiber-reinforced concrete. *Mechanics of Composite Materials and Structures* 8(1): 29–45.

Barros JOA, Cunha VMCF, Ribeiro AF, et al. (2005) Post-cracking behaviour of steel fibre reinforced concrete. *Materials and Structures* 38(1): 47–56.
Bencardino F, Rizzuti L, Spadea G, et al. (2010) Experimental evaluation of fiber reinforced concrete fracture properties. *Composites Part B: Engineering* 41(1): 17–24.
Bosco C and Carpinteri A (1995) Discontinuous constitutive response of brittle matrix fibrous composites. *Journal of the Mechanics and Physics of Solids* 43(2): 261–274.
Carpinteri A (1981) A fracture mechanics model for reinforced concrete collapse. In: *Proceedings of the IABSE colloquium on advanced mechanics of reinforced concrete*, 17–30, Delft, June 2–4, 1981.
Carpinteri A (1984) Stability of fracturing process in RC beams. *Journal of Structural Engineering* 110(3): 544–558.
Carpinteri A and Accornero F (2019) The bridged crack model with multiple fibers: Local instabilities, scale effects, plastic shake-down, and hysteresis. *Theoretical and Applied Fracture Mechanics* 104: 102351.
Carpinteri A and Accornero F (2020) Residual crack opening in fiber-reinforced structural elements subjected to cyclic loading. *Strength, Fracture and Complexity* 12(2–4): 63–74.
Carpinteri A and Carpinteri A (1984) Hysteretic behavior of RC beams. *Journal of Structural Engineering* 110(9): 2073–2084.
Carpinteri A and Massabò R (1996) Bridged versus cohesive crack in the flexural behavior of brittle-matrix composites. *International Journal of Fracture* 81(2): 125–145.
Carpinteri A and Massabò R (1997a) Continuous vs discontinuous bridged crack model of fiber-reinforced materials in flexure. *International Journal of Solids and Structures* 34(18): 2321–2338.
Carpinteri A and Massabò R (1997b) Reversal in failure scaling transition of fibrous composites. *Journal of Engineering Mechanics* 123(2): 107–114.
Carpinteri A and Accornero F (2021) Dimensional analysis of critical phenomena: Self weight failure, turbulence, resonance, fracture. *Physical Mesomechanics* 24(4): 459–463.
Carpinteri A, Accornero F and Rubino A (2022) Scale effects in the post-cracking behaviour of fibre-reinforced concrete beams. *International Journal of Fracture* 240(1): 1–16.
Colombo M, Conforti A, Di Prisco M, et al. (2023) The basis for ductility evaluation in SFRC structures in MC2020: an investigation on slabs and shallow beams. *Structural Concrete* 24(4): 4406–4423.
Dancygier AN and Savir Z (2006) Flexural behavior of HSFRC with low reinforcement ratios. *Engineering Structures* 28(11): 1503–1512.
Di Prisco M, Plizzari G and Vandewalle L (2009) Fibre reinforced concrete: New design perspectives. *Materials and Structures* 42(9): 1261–1281.
Fantilli AP, Chiaia B and Gorino A (2016) Fiber volume fraction and ductility index of concrete beams. *Cement and Concrete Composites* 65: 139–149.
FIB (Federation International du Bèton) (2012) *Model Code 2010 – Final Draft*. Vol. 1. Switzerland, Lausanne, FIB Bulletin, 65.
Gorino A and Fantilli A (2020) Scaled approach to designing the minimum hybrid reinforcement of concrete beams. *Materials* 13(22): 5166.
Hillerborg A, Modéer M and Petersson P-E (6, 1976) Analysis of crack formation and crack growth in concrete by means of fracture mechanics and finite elements. *Cement and Concrete Research* 6(6): 773–781.
Holschemacher K, Mueller T and Ribakov Y (2010) Effect of steel fibres on mechanical properties of high-strength concrete. *Materials & Design (1980–2015)* 31(5): 2604–2615.
Jenq YS and Shah SP (1985) A fracture toughness criterion for concrete. *Engineering Fracture Mechanics* 21(5): 1055–1069.
Li VC, Wang Y and Backer S (1990) Effect of inclining angle, bundling and surface treatment on synthetic fibre pull-out from a cement matrix. *Composites* 21(2): 132–140.
Liao L, de l, Fluente A, Cavalaro, et al. (2016) Design procedure and experimental study on fibre reinforced concrete segmental rings or vertical shafts. *Materials & Design* 92: 590–601.
Meda A, Minelli F and Plizzari GA (2012) Flexural behaviour of RC beams in fibre reinforced concrete. *Composites Part B: Engineering* 43(8): 2930–2937.

Mertol HC, Baran E and Bello HJ (2015) Flexural behavior of lightly and heavily reinforced steel fiber concrete beams. *Construction and Building Materials* 98: 185–193.

Mobasher B, Bakhshi M and Barsby C (2014) Backcalculation of residual tensile strength of regular and high performance fiber reinforced concrete from flexural tests. *Construction and Building Materials* 70: 243–253.

Mobasher B, Yao Y and Soranakom C (2015) Analytical solutions for flexural design of hybrid steel fibre reinforced concrete beams. *Engineering Structures* 100: 164–177.

Naaman AE (2008) High performance fiber reinforced cement composites. In: Chung DDL (ed.) *Vol. 1*: *High Performance Construction Material*s (Caijun Shi and Mo YL, eds) *Engineering Materials for Technological Needs*. Singapore: World Scientific Publishing Co. Pte. Ltd, pp. 91–153.

Nguyen W, Bandelt MJ, Trono W, et al. (2019) Mechanics and failure characteristics of hybrid fiber-reinforced concrete (HyFRC) composites with longitudinal steel reinforcement. *Engineering Structures* 183: 243–254.

Ning X, Ding Y, Zhang F, et al. (2015) Experimental study and prediction model for flexural behaviour of reinforced SCC beam containing steel fibres. *Construction and Building Materials* 93: 644–653.

RILEM TC 162-TDF (2002) Test and design method for steel fibre reinforce concrete. Design of steel fibre reinforced concrete using the σ–w method: principles and applications. *Materials and Structures* 35(5): 262–278.

RILEM TC 162-TDF (2003) Test and design method for steel fibre reinforce concrete. σ–ε design method. Final recommendation. *Materials and Structures* 36(262): 560–567.

Robins P, Austin S and Jones P (2003) Spatial distribution of steel fibres in sprayed and cast concrete. *Magazine of Concrete Research* 55(3): 225–235.

Rubino A, Accornero F and Carpinteri A (2023) Flexural behaviour and minimum reinforcement condition in hybrid-reinforced concrete beams. *Structural Concrete* 24(4): 4767–4778.

Shao Y and Billington SL (2020) Flexural performance of steel-reinforced engineered cementitious composites with different reinforcing ratios and steel types. *Construction and Building Materials* 231: 117159.